Cerebral Cortex October 2011;21:2261-2271
doi:10.1093/cercor/bhq293
Advance Access publication February 24, 2011

Microstructure of Frontoparietal Connections Predicts Cortical Responsivity and Working Memory Performance

A. Z. Burzynska[1], I. E. Nagel[1,2], C. Preuschhof[2], S.-C. Li[1], U. Lindenberger[1], L. Bäckman[1,3] and H.R. Heekeren[1,2,4]

[1]Max Planck Institute for Human Development, Lentzeallee 94, 14195 Berlin, Germany, [2]Department of Education and Psychology, Freie Universität Berlin, 14195 Berlin, Germany, [3]Aging Research Center, Karolinska Institute, Gävlegatan 16, SE-11330, Stockholm, Sweden and [4]Max Planck Institute for Human Cognitive and Brain Sciences, Stephanstraße 1a, 04103 Leipzig, Germany

Address correspondence to A. Z. Burzynska. Email: burzynska@mpib-berlin.mpg.de.

We investigated how the microstructure of relevant white matter connections is associated with cortical responsivity and working memory (WM) performance by collecting diffusion tensor imaging and verbal WM functional magnetic resonance imaging data from 29 young adults. We measured cortical responsivity within the frontoparietal WM network as the difference in blood oxygenation level–dependent (BOLD) signal between 3-back and 1-back conditions. Fractional anisotropy served as an index of the integrity of the superior longitudinal fasciculi (SLF), which connect frontal and posterior regions. We found that SLF integrity is associated with better 3-back performance and greater task-related BOLD responsivity. In addition, BOLD responsivity in right premotor cortex reliably mediated the effects of SLF integrity on 3-back performance but did not uniquely predict 3-back performance after controlling for individual differences in SLF integrity. Our results suggest that task-related adjustments of local gray matter processing are conditioned by the properties of anatomical connections between relevant cortical regions. We suggest that the microarchitecture of white matter tracts influences the speed of signal transduction along axons. This in turn may affect signal summation at neural dendrites, action potential firing, and the resulting BOLD signal change and responsivity.

Keywords: DTI, fMRI, multimodal, n-back, superior longitudinal fasciculi

Introduction

Working memory (WM) involves holding information "online" for active monitoring and manipulation in the absence of external cues (Baddeley 2003; D'Esposito 2007). WM relies on a distributed frontoposterior network including lateral prefrontal cortex (PFC), supplementary motor area (SMA), premotor cortex (PMC), and posterior parietal cortex (PPC; Jonides et al. 1993, 1997; Salmon et al. 1996; Miller and Cohen 2001; Owen et al. 2005; Rajah and D'Esposito 2005; D'Esposito 2007). In these regions, changes in blood oxygenation level–dependent (BOLD) signal increase with WM load (Barch et al. 1997; Braver et al. 1997; Klingberg et al. 1997; Manoach et al. 1997; Callicott et al. 1999; Rypma et al. 1999; Nagel et al. 2009, 2010). We have shown that individuals differ in the extent to which the BOLD response is adjusted as a function of increasing WM demand (Nagel et al. 2009, 2010). Critically, Nagel et al. (2009, 2010) demonstrated that this load-dependent modulation of the BOLD signal predicted performance in the most challenging WM condition.

However, the relation between individual differences in WM capacity and cortical BOLD responsivity to increasing WM load is not well understood. Performance-related BOLD responsivity has been shown to relate to local cortical processing (e.g., Achard and Bullmore 2007), dopaminergic neurotransmission (Bäckman et al. 2009; Fischer et al. 2010), and local cortical volume (Brassen et al. 2009). Here, we focus on another, less explored mechanism of BOLD responsivity: We predicted that individual differences in the microstructure of the anatomical connections within the WM network influence cortical responsivity and performance.

The few studies that have combined measures of white matter microstructure (using diffusion tensor imaging, DTI) and cortical activity (using functional magnetic resonance imaging, fMRI) provide support for the hypothesis that individual differences in the microstructure of anatomical connections between relevant brain areas are related to cortical function. In an exploratory voxel-based analysis, Nagy et al. (2004) showed that fractional anisotropy (FA) in the frontal lobe and in a region between the superior frontal and parietal cortices correlated with spatial WM scores in a group of children. Moreover, these FA values were positively correlated with the BOLD response in superior frontal sulcus and intraparietal cortex (Olesen et al. 2003). The correlation may have reflected the simultaneous maturation of white and gray matter as WM scores no longer correlated with FA values or the BOLD response after statistically controlling for individual differences in chronological age. Nordahl et al. (2006) related white matter degeneration, measured as white matter hyperintensities (WMHs), to the magnitude of prefrontal activity during a verbal WM task in a group of elderly individuals. Global WMH volume correlated negatively with right dorsal PFC activity, and greater dorsal PFC WMH volume was associated with decreased activity in the PPC and anterior cingulate cortex. Finally, in a study on schizophrenic patients and controls, Schlösser et al. (2007) showed that the patients had reduced FA in the right medial temporal lobe and in the right frontal lobe. During a Sternberg WM task, patients showed reduced activation in prefrontal, superior parietal, and occipital regions. Importantly, greater frontal FA was related to greater BOLD activation in prefrontal and occipital regions in patients.

Taken together, these findings on development, aging, and disease suggest that integrity of white matter connections is related to greater changes in activity in task-relevant cortical regions. However, the mechanisms and regional specificity of white–gray matter relations in these samples with maturing or altered brain structure and function may not generalize to the central nervous system of normal young adults.

By combining fMRI and DTI in a group of healthy young adults, our goal in this study was to delineate the relations

between white matter microstructure, WM load-related changes in BOLD signal, and WM performance. We aimed to study the possible mechanisms underlying the adaptation of the BOLD signal change to increasing WM task demand (BOLD responsivity). The more general question was how is BOLD responsivity in certain cortical regions related to white matter microstructure interconnecting these regions? Specifically, we asked whether 1) the effect of white matter microstructure on WM performance is mediated by BOLD responsivity; and 2) the relation between BOLD responsivity and WM performance can be accounted for individual differences in white matter microstructure.

To address these questions, we measured brain activity during a verbal WM task (1-back, 2-back, and 3-back) in 29 younger adults. By using this parametric design, we were able to measure cortical responsivity, operationalized as the difference in BOLD signal between the 3-back and 1-back conditions. Compared with the more frequently used difference between baseline and task-related activation, this contrast reflects the load-dependent change in cortical activity, circumventing the problem of individual differences in absolute magnitude and extent of the hemodynamic response. Also, for the purpose of the present study, a blocked fMRI design is advantageous because it increases the statistical power for detecting associations among structural, functional, and behavioral measures relative to an event-related design.

The functional network involved in performing *n*-back includes prefrontal and parietal regions, in addition to visual areas (Jonides et al. 1993, 1997; Miller and Cohen 2001; Owen et al. 2005; D'Esposito 2007; Nagel et al. 2009, 2010). The superior longitudinal fasciculi (SLF) are the primary and direct pathways providing the bidirectional information transfer between the frontal and the parietal cortices (Petrides and Pandya 1984; Schmahmann and Pandya 2006). Therefore, we hypothesized that individual differences in the SLF would be related to BOLD responsivity in the *n*-back functional network and to WM performance.

To assess the microstructure of the SLF, we employed DTI, which permits inferences about white matter microscopic cellular architecture in vivo by quantifying the magnitude and directionality of diffusion of water within a tissue (Pierpaoli and Basser 1996; Pierpaoli et al. 1996). FA is a measure of the directional dependence of diffusion (Basser 1995) and can take values between 0 (isotropic diffusion) and 1 (perfectly anisotropic diffusion). Tract-specific and individual differences in FA are thought to reflect differences in axon volume fraction, distribution of axon diameters, spacing and coherence, and the degree of myelination or fraction of myelinated axons (Pierpaoli et al. 1996; Beaulieu 2002; Sen and Basser 2005). The microscopic architecture of white matter, in particular the axon caliber and the myelin sheath thickness, influences the signal conduction speed along the axons and, therefore, synchronization of nervous signals (Fields 2008).

Our study was guided by 4 main hypotheses. First, we predicted that the speed of information transfer between core regions in the WM network should be related to WM performance, especially at high levels of task difficulty. Thus, we expected that greater white matter integrity (FA) in the SLF would be related to better performance in the 3-back condition. Second, we expected that more efficient signal transfer along white matter fibers should predict individuals' ability to upregulate cortical activation with increasing load. Hence, we hypothesized that greater integrity of the SLF should be related to higher BOLD responsivity within the WM network. Third, we expected that the effect of greater white matter integrity on 3-back performance would be mediated by the increase in BOLD signal from 1-back to 3-back in task-relevant regions. Fourth, and conversely, we also expected that the association between BOLD responsivity and WM performance would be attenuated or eliminated after statistically controlling for individual differences in white matter microstructure.

Materials and Methods

Participants

Twenty-nine right-handed psychiatrically and neurologically healthy adults with normal or corrected-to-normal vision participated in the study (age 19–31 years, mean ± standard deviation [SD] = 24.2 ± 3.1, 15 female, years of education = 16.3 ± 3.1). All subjects showed age-relevant performance levels on measures of processing speed (63.9 ± 11.2 items completed in Digit Symbol Substitution) and verbal knowledge (18.2 ± 5.0 correct responses on the Spot-a-Word task; e.g., Shing et al. 2009) carried out during the DTI session. All statistical analyses were performed using SPSS (v. 16, SPSS Inc.).

The Ethics Committee of the Charité University Medicine Berlin approved the study, and written informed consent was obtained from all participants. Participants received financial reimbursement.

Functional MRI

n-back Task

Participants performed a letter *n*-back task with parametric manipulation of WM load. A series of letters was presented and the task was to compare the currently presented letter with the one seen 1, 2, or 3 letters earlier (1-, 2-, and 3-back conditions, respectively). Each trial began with 5000 ms presentation of the condition cue (1-, 2-, or 3-back). Each letter stimulus was presented for 1500 ms, separated by 500 ms fixation periods. Responses were given by button press. Prior to entering the scanner, participants were verbally instructed about the task, then practiced 3 runs, and received feedback on their performance.

n-back performance was assessed by the percent of correct responses (accuracy). To assess load-dependent effects on accuracy, we used repeated-measures analysis of variance (ANOVA) with task load (1-, 2-, 3-back) as a within-subjects factor.

fMRI Data Acquisition

Whole-brain functional MRI data were collected with a 1.5 T Siemens Vision MRI system with a standard echo planar imaging (EPI) sequence (time repetition/time echo [TR/TE] = 2500/40 ms, flip angle 90°, 4 × 4 × 4 mm voxel volume, interslice gap 15% of the slice thickness, 26 slices acquired in ascending order ca. axial to the bicommissural plane). Three dummy volumes preceded each of the 3 experimental runs to achieve a steady state of tissue magnetization. Each run lasted about 5 min. Two structural scans (proton density–weighted sequence: TR/TE = 4350/15 ms; flip angle 180°; 252 × 256 matrix; 1 × 1 × 4 mm voxel size, and a sagittally oriented high resolution T_1-weighted sequence: TR/TE = 20/5 ms; flip angle 30°; matrix 256 × 256; voxel size 1 mm^3) were acquired in the same orientation as the functional EPIs to aid co-registration of the functional images.

fMRI Data Analysis

fMRI data were analyzed with FSL 4.1 (FMRIB's Software Library, http://www.fmrib.ox.ac.uk/fsl; Smith et al. 2004). Preprocessing included: slice time and motion correction with spatial smoothing (8 mm full-width at half maximum Gaussian kernel), high-pass filtering (sigma = 108 s), and modeling of intrinsic autocorrelations using prewhitening. Three regressors were used with each modeling one of the load conditions (1-, 2-, 3-back) and a fourth regressor was used to model the

appearance of the cue indicating the condition before each block. Regressors were convolved with a hemodynamic response function (gamma variate). Registration to high resolution and standard images was carried out using FLIRT (Jenkinson et al. 2002; Jenkinson and Smith 2001). Contrast images were computed for each condition per subject. These images were then spatially normalized and transformed into standard space (Jenkinson et al. 2002). Group effects were computed using the transformed contrast images in a mixed-effects general linear model treating subjects as random. We used a threshold of $z > 3.1$ ($P < 0.001$, minimum cluster size = 20 voxels) for whole-brain analyses.

To investigate the load-dependent increase in brain activity, we conducted region-of-interest (ROI)-based analyses within task-relevant regions. We calculated a contrast comparing WM task-related activation (mean of 1-, 2-, and 3-back) to fixation baseline and then defined 8 mm spherical ROIs around the peak activation in regions where changes in BOLD signal were significant ($P < 0.005$ uncorrected, Fig. 1). These regions included bilateral anterior frontopolar cortex (AFPC, Brodmann area [BA] 10), DLPFC (dorsolateral PFC, BA 9/46), VLPFC (ventral–lateral PFC, BA 44/45), SMA (medial BA 6 and 8), PMC (BA 6), and PPC (BA 7). For each ROI and subject, we extracted mean percent signal change for the 1- and 3-back conditions. We next computed BOLD responsivity scores as the signal change at 3-back minus signal change at 1-back.

Diffusion Tensor Imaging

DTI Data Acquisition

For logistic reasons, DTI images could not be acquired on the Siemens Vision scanner used for fMRI. Therefore, diffusion-weighted images were acquired on a scanner with the same field strength (Siemens Sonata 1.5 T, 40 mT/m gradients and 200 T/m/s slew rates; Siemens). Analysis of both fMRI and DTI data was based on ROI and therefore did not require co-registration of images with different MRI contrast and acquired on different scanners. Due to limited availability of the scanning time, DTI data were collected after the acquisition of the fMRI data. The average time interval between the 2 measurement occasions was 57 days (range = 3–240 days; SD = 66 days). DTI images were obtained parallel to the anterior–posterior commissure plane with no interslice gap. Eddy current-induced image distortions were minimized by using a twice-refocused spin echo single-shot EPI sequence to acquire DTI data (Reese et al. 2003), with TR/TE = 8500/96 ms, 128 × 128 matrix, 2.5 mm^2 in-plane resolution, and receiver bandwidth of 1502 Hz, comprising fifty-two 2.5-mm thick slices. The protocol consisted of a set of 12 noncollinear diffusion-weighted acquisitions, with b value = 1000 s/mm^2 and a T_2-weighted, b value = 0 s/mm^2 acquisition, each repeated 4 times.

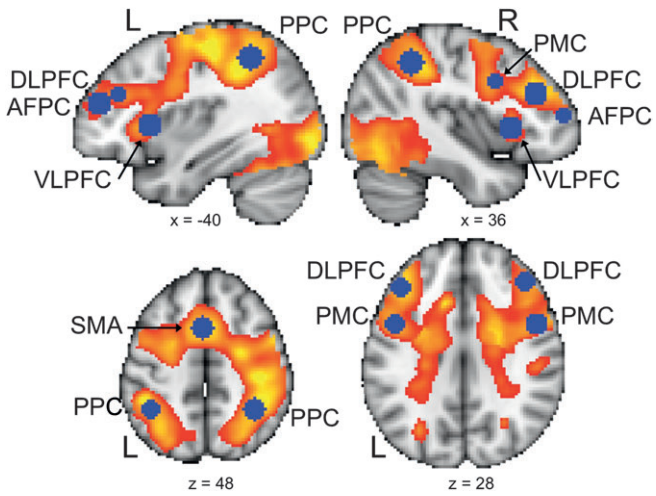

Figure 1. *n*-back functional network in 29 younger adults. In red–yellow: mean of BOLD signal increase during 1-back, 2-back, and 3-back condition, compared with fixation baseline, $z > 2.6$, uncorrected. In blue: 8 mm spherical ROIs around peak voxels ($P < 0.005$). L: left hemisphere, R: right hemisphere. *x*, *z*: coordinates in the MNI space (mm).

Analysis of DTI Data

DTI data were processed using the FSL 4.1 Diffusion Toolbox (FDT: http://www.fmrib.ox.ac.uk/fsl) in a standard multistep procedure, including 1) motion and eddy current correction of the images and b - vectors rotation, 2) removal of the skull and nonbrain tissue using the Brain Extraction Tool (Smith 2002), and 3) voxel-by-voxel calculation of the diffusion tensors. Using the diffusion tensor information, FA maps were computed using DTIFit within the FDT.

Center-of-tract FA values of the main white matter pathways were transformed to standard space for each participant using TBSS v.1.2 (Smith et al. 2006, 2007), a toolbox within FSL (Smith et al. 2004), and included 1) nonlinear alignment of each participant's FA volume to the 1 × 1 × 1 mm^3 standard Montreal Neurological Institute (MNI152) space via the FMRIB58_FA template using the FMRIB's Nonlinear Registration Tool (FNIRT, Rueckert et al. 1999; http://www.doc.ic.ac.uk/~dr/software), 2) calculation of the mean of all aligned FA images, 3) creation of the WM "skeleton" (a representation of WM tracts common to all subjects) by perpendicular nonmaximum suppression of the mean FA image and setting the FA threshold to 0.25, and 4) perpendicular projection of the highest FA value (local center of the tract) onto the skeleton, separately for each subject.

ROI Analysis

We expected SLF to be the key white matter tract involved in WM performance as its fibers link the association parietal cortices to the frontal lobe (Schmahmann and Pandya 2006). Tracing studies in nonhuman primates have shown that SLF consists of 3 separate components: SLF I connecting medial PPC and the caudal superior parietal lobule (BA 7) to SMA and PMC (medial and dorsal part of the superior frontal gyrus; BA 6, 8, 9); SLF II originating in the inferior parietal lobule (BA 39) and regions of the ventral bank of the interparietal sulcus (BA 7) and terminating in the dorsal PMC (BA 6), SMA (BA 8), and DLPFC (BA 9 and 46); and SLF III connecting the rostral part of the inferior parietal lobule (BA 39) and parietal operculum (BA 40) to the ventral PMC (BA 6), VLPFC (BA 44; Petrides and Pandya 1984; Schmahmann and Pandya 2006). The core of these tracts have been identified and segmented in a DTI tractography study in humans; however, the origin and termination of the subdivisions could not be reliably assessed with DTI and hence were inferred from nonhuman data (Makris et al. 2005). Therefore, we placed the SLF ROI on the TBSS white matter skeleton so that it represented the very central part of the SLF (Fig. 2*A*), mainly the SLF II and to lesser extent SLF III (Makris et al. 2005). SLF II is much larger (i.e., thicker) than SLF I and III (Makris et al. 2005) and can therefore be reliably identified on the TBSS skeleton, as shown in a previous TBSS study (Karlsgodt et al. 2008) and with the help of the DTI white matter atlas (Mori et al. 2005). Most importantly, SLF II is thought to serve as a conduit for the neural systems subserving visual awareness and maintenance of attention (Schmahmann and Pandya 2006), which are expected to play a role in WM performance. Damage to the SLF II and SLF III has been related to impairments in WM due to disruption of the connections of the DLPFC (BA 46) and VLPFC (BA 44; Preuss and Goldman-Rakic 1989; Petrides and Pandya 2002). In contrast, SLF I is thought to be involved mainly in regulation of higher aspects of motor behavior and initiation of motor activity (Schmahmann and Pandya 2006). Finally, to ensure that the voxels sampled onto the white matter skeleton were derived from the same structures in all participants, we deprojected the SLF ROI into individual FA maps in MNI space. Figure 2*B* shows deprojected SLF ROI in 2 representative subjects.

In addition, we specified a control ROI, where fibers are not expected to be involved in the core WM network, namely, a subregion of the corpus callosum at the level of the primary somatosensory cortex (region 4 of corpus callosum, Fig. 2*C*; Hofer and Frahm 2006). Finally, we extracted mean FA values from the left and right SLF, from the control ROI, and the total WM skeleton.

We then z-transformed the BOLD responsivity, 3-back accuracy, and FA values. z-scores larger than ± 2 SD were considered outliers and were excluded from the analyses. This resulted in the following sample

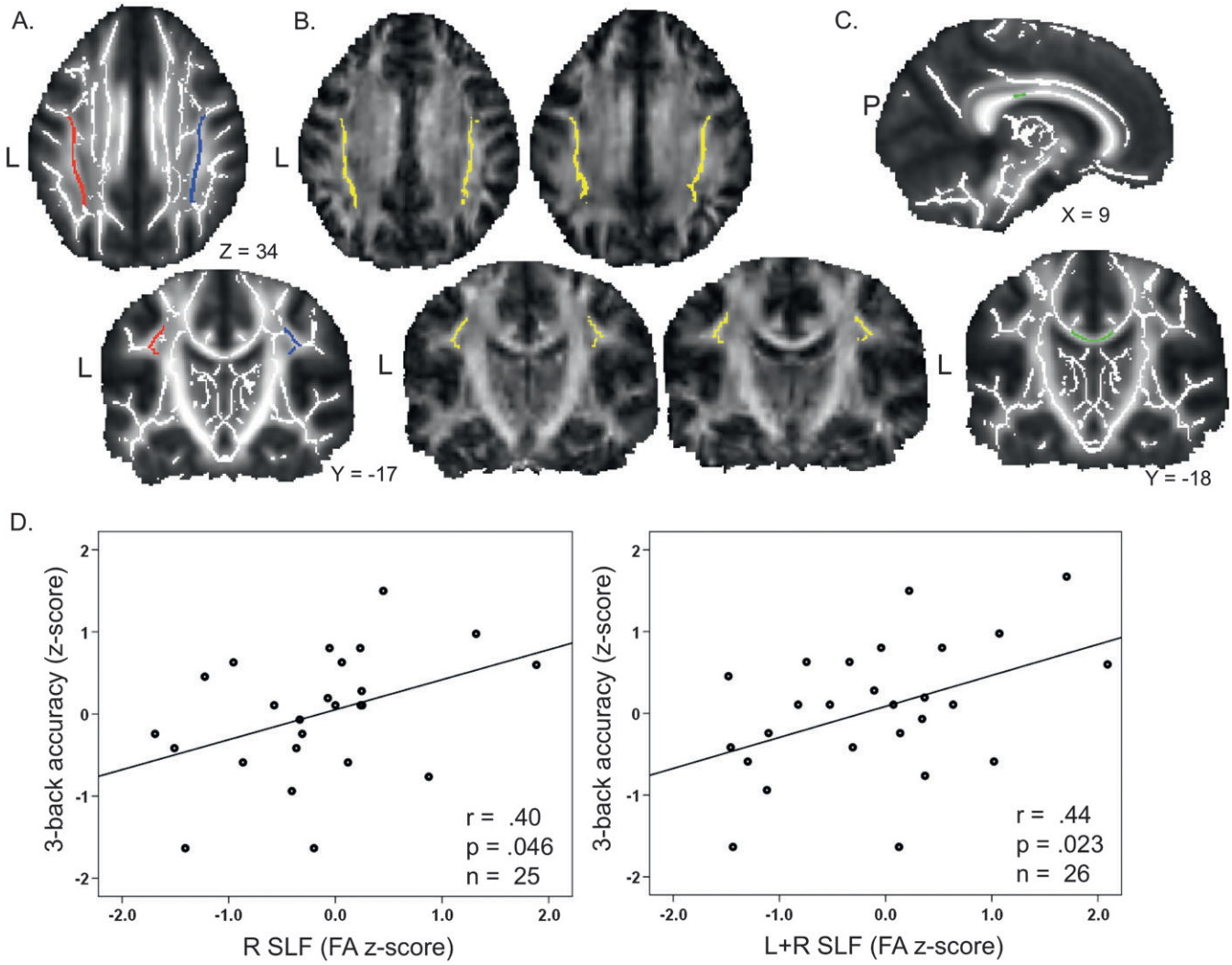

Figure 2. (*A*) Definition of the SLF ROI. Blue: right SLF, red: left SLF, overlaid on mean FA image of 29 participants in standard MNI space. (*B*) Skeleton-space voxels from the SLF ROI of 4 different participants, de-projected onto subjects' FA image in standard MNI space (nonlinearly registered). (*C*) Definition of the control ROI: region 4 of the corpus callosum (Hofer and Frahm 2006), containing primary somatosensory interhemispheric connections. *x*, *y*, *z*: coordinates in the MNI space (mm). L: left, P: posterior. (*D*) Correlation of FA in SLF with accuracy in the 3-back condition.

sizes for different measures: BOLD responsivity ($n_{\text{L DLPFC}} = 25$, $n_{\text{R DLPFC}} = 27$, $n_{\text{L VLPFC}} = 28$, $n_{\text{R VLPFC}} = 28$, $n_{\text{L AFPC}} = 26$, $n_{\text{R AFPC}} = 26$, $n_{\text{SMA}} = 27$, $n_{\text{L PMC}} = 27$, $n_{\text{R PMC}} = 25$, $n_{\text{L PPC}} = 27$, $n_{\text{RPPC}} = 27$), 3-back accuracy ($n = 27$), FA values ($n_{\text{FA skel}} = 28$, $n_{\text{FA L + R SLF}} = 28$, $n_{\text{R SLF}} = 27$, $n_{\text{L SLF}} = 29$, $n_{\text{region 4 cc}} = 27$).

Relating White Matter Microstructure to BOLD Responsivity and Performance

To examine the relation between white matter microstructure of the SLF and BOLD responsivity within the *n*-back functional network, we correlated FA with BOLD responsivity within each hemisphere, as well as FA of the total (i.e., bilateral) SLF with BOLD responsivity of each ROI. Next, we correlated 3-back accuracy with BOLD responsivity and FA values.

To check how specific the result was to FA of the SLF, we performed a linear hierarchical regression analysis, where BOLD responsivity was the dependent variable, whole white matter FA was entered as first, and SLF FA was entered as the second independent variable.

We specified a path model to examine relations among white matter microstructure, BOLD responsivity, and WM performance. A mediator model typically consists of an independent (or exogenous) variable, a mediator variable, and a dependent variable. Both the independent and the mediator variables are assumed to influence the dependent variable. The independent variable influences the dependent variable both directly and indirectly through its effect on the mediator variable. Hence, what distinguishes the independent variable from the mediator variable is that the independent variable is assumed to influence both the mediator and the dependent variable, whereas the mediator variable is assumed to influence the dependent variable but not the independent variable. If we map these statistical relations onto the substantive assumptions that guide this article, then FA as a measure of white matter microstructure is the independent variable because we assume that it influences both BOLD responsivity and WM performance (Note: Reverse effects of BOLD and FA are also possible. For instance, extended periods of coactivation may shape white matter connections, at least early in ontogeny. However, for the present sample and measurements, the assumption of a directional effect of FA on BOLD responsivity appears justified.) We also assume that BOLD responsivity influences WM performance and is influenced by FA. These 2 relations put BOLD responsivity in the position of a mediator between FA and WM performance. Based on these considerations, the mediator model that properly expresses our substantive considerations has FA as the independent variable, the BOLD responsivity as the mediator, and WM as the dependent variable. In terms of causal relations, this statistical model represents the assumptions that FA and BOLD responsivity function as distal and proximal causes of WM performance, respectively

(see Fig. 5). We used bootstrapping procedures to minimize problems related to small sample size (cf. MacKinnon 2000; MacKinnon et al. 2004). Bootstrapping statistics make no a priori assumptions about the distribution of the paths *a*, *b*, and their product *ab* (indirect effect; Preacher and Hayes 2008a, 2008b). The analysis was implemented using the INDIRECT macro for SPSS developed by Preacher and Hayes (www.quantypsy.org). In brief, an empirical estimation of the sampling distribution of the product of the *a* and *b* paths was generated by taking a new sample of size *n* with replacement from the available sample. Then the *a* and *b* estimates were used to calculate ab^*, the indirect effect of FA on WM performance, in a single resample of size *n* from the original data. This process was repeated *k* times (i.e., $k = 5000$ bootstrap resamples). The distribution of ab^* served as an empirical nonparametric approximation of the sampling distribution of the indirect effect. The 95% bias corrected and accelerated confidence interval (corrected for both median bias and skew; Efron 1987) of the indirect effect are derived by sorting the ab^* values from low to high and defining the lower ($0.5 \times (1 - 0.95) \times 5000 = 125$th value in the sorted ab^* distribution) and upper ($(1 + 0.5 \times (1 + 0.95) \times 5000 = 4876$th value) bounds. The null hypothesis of no indirect effect was tested by determining whether zero was within the confidence interval. If this is not the case, it can be claimed that the indirect effect is different from zero.

Finally, we investigated whether BOLD responsivity reliably predicted unique amounts of variance in 3-back performance after controlling for individual differences in FA of the SLF. To this end, we performed a stepwise multiple regression analysis with FA as the first predictor variable, BOLD responsivity in the R PMC as the second predictor variable, and 3-back accuracy as the dependent variable. If the relation between BOLD responsivity and WM performance is primarily dependent on the microstructure of the underlying white matter, then R PMC BOLD responsivity should no longer be a significant predictor of 3-back accuracy when statistically controlling for white matter integrity. The information whether BOLD responsivity predicts WM performance after controlling for individual differences in FA could also have been derived on the basis of our conceptually preferred model by setting the path from the BOLD response to WM performance to zero and testing whether this constraint is associated with a significant decrement in predicted variance in the dependent variable. Unfortunately, the bootstrapping mediation routine by Preacher and Hayes (2008a, 2008b) does not allow for setting the path from the mediator to the dependent variable to zero, which is why we used hierarchical regression analysis to obtain this specific piece of information.

Results

Greater BOLD Responsivity Is Related to Better WM Performance at High Load

First, a repeated-measures ANOVA revealed that the main effect of task difficulty for accuracy, $F_{2,56} = 47.53$, $P < 0.001$, $\eta^2 = 0.63$, was statistically reliable, indicating that accuracy decreased linearly with rising task difficulty from 1- to 3-back (Fig. 3*B*). Second, BOLD signal change increased linearly up to the highest load level (3-back) in most ROIs (R AFPC $F_{2,56} = 3.68$, $P = 0.032$, $\eta^2 = 0.116$; L AFPC $F_{2,56} = 6.10$, $P = 0.004$, $\eta^2 = 0.179$; R DLPFC $F_{2,56} = 7.68$, $P = 0.001$, $\eta^2 = 0.215$; L DLPFC $F_{2,56} = 7.23$, $P = 0.002$, $\eta^2 = 0.205$; L VLPFC $F_{2,56} = 3.37$, $P = 0.042$, $\eta^2 = 0.107$; SMA $F_{2,56} = 5.01$, $P = 0.010$, $\eta^2 = 0.152$; R PMC $F_{2,56} = 4.40$, $P = 0.017$, $\eta^2 = 0.136$; L PPC $F_{2,56} = 7.38$, $P = 0.001$, $\eta^2 = 0.208$) and at trend level in R PPC ($F_{2,56} = 2.76$, $P = 0.072$, $\eta^2 = 0.090$), and L PMC ($F_{2,56} = 2.44$, $P = 0.096$, $\eta^2 = 0.080$), but was nonsignificant in R VLPFC ($F_{2,56} = 2.27$, $P = 0.113$, $\eta^2 = 0.075$; for illustration, see Fig. 3*A*). Third, greater BOLD responsivity (signal change at the 3-back minus 1-back condition) in the R PMC ($r = 0.505$ $P = 0.012$ $n = 24$) and at trend level in the L VLPFC ($r = 0.373$ $P = 0.060$ $n = 26$) was related to higher 3-back accuracy (Fig. 3*C*).

Higher Integrity of the SLF White Matter Is Related to Better WM Performance at High Load

The mean FA values ± SD in the SLF were $FA_{L\ SLF} = 0.47 \pm 0.03$, $FA_{R\ SLF} = 0.50 \pm 0.03$, $FA_{L+R\ SLF} = 0.48 \pm 0.03$. The mean FA in the somatosensory region of the corpus callosum was $FA_{reg4cc} = 0.68 \pm 0.05$ and in the whole skeleton $FA_{skel} = 0.47 \pm 0.01$. Importantly, we observed no relation between chronological age and 3-back accuracy, FA_{SLF}, FA_{reg4cc}, and BOLD responsivity in this sample of young adults. Therefore, age was not included in further analyses.

We predicted that microstructure in the SLF is related to *n*-back performance at the highest WM load (3-back). Correlation analysis revealed that, indeed, higher $FA_{R\ SLF}$ ($r = 0.40$, $P = 0.046$, $n = 25$) and $FA_{L+R\ SLF}$ ($r = 0.44$, $P = 0.023$, $n = 26$) but not the control FA_{reg4cc} ($r = 0.31$, $P = 0.128$, $n = 26$) and FA_{skel} ($r = 0.03$, $P = 0.887$, $n = 26$) was related to higher 3-back accuracy. Scatter plots of the FA–WM relationships are displayed in Figure 2*D*.

Greater BOLD Responsivity Is Related to Higher SLF Integrity

To investigate associations between white matter microstructure and cortical responsivity, we correlated FA with BOLD responsivity. We found that higher FA in SLF, but not in the control region 4 of the corpus callosum, was related to higher BOLD responsivity within the *n*-back functional network (for details, see Table 1). Figure 4 displays representative scatterplots.

Next, we performed multiple hierarchical regression analyses to test whether individual differences in FA_{SLF} were uniquely related to individual differences in BOLD responsivity after statistically controlling for individual differences in FA_{skel}. The change statistics were significant for models with BOLD responsivity in R PMC ($FA_{R\ SLF}$ $R^2_{change} = 0.195$, $F_{change}\ (1/20) = 5.092$, $P = 0.035$) and R VLPFC ($FA_{L+R\ SLF}$ $R^2_{change} = 0.219$, $F_{change}\ (1/23) = 6.47$, $P = 0.018$) as outcome variables, showing that FA in the SLF was an important predictor of BOLD responsivity beyond FA_{skel}.

BOLD Responsivity Statistically Mediates the Effect of SLF Microstructure on WM Performance at High Load

Next, we examined whether the data are consistent with the hypothesis that BOLD responsivity mediates the effect of white matter microstructure on 3-back performance. We used bootstrapping to determine the confidence intervals of indirect effects of BOLD responsivity in the R PMC in 2 models, one with FAR_{SLF} as independent variable and the other with $FA_{L+R_{SLF}}$ (Fig. 5). We considered only BOLD responsivity in the R PMC as it was significantly related to 3-back performance.

Table 2 summarizes the coefficients, point estimates, and 95% bias-corrected and accelerated bootstrap confidence intervals of the mediation models. Our results indicate that the difference between the total and direct effect of $FA_{L+R\ SLF}$ (but not of $FA_{R\ SLF}$) on 3-back accuracy was reliable as zero was outside of the confidence intervals. In other words, the effect of R PMC BOLD as a potential mediator of the effects of $FA_{L+R\ SLF}$ on 3-back accuracy was significantly different from zero.

BOLD Responsivity Does Not Reliably Predict WM Performance at High Load Beyond SLF Microstructure

Finally, we tested whether the predictive effect of BOLD responsivity on 3-back performance was limited to its role as a mediator of the effect of FA on WM performance. For this

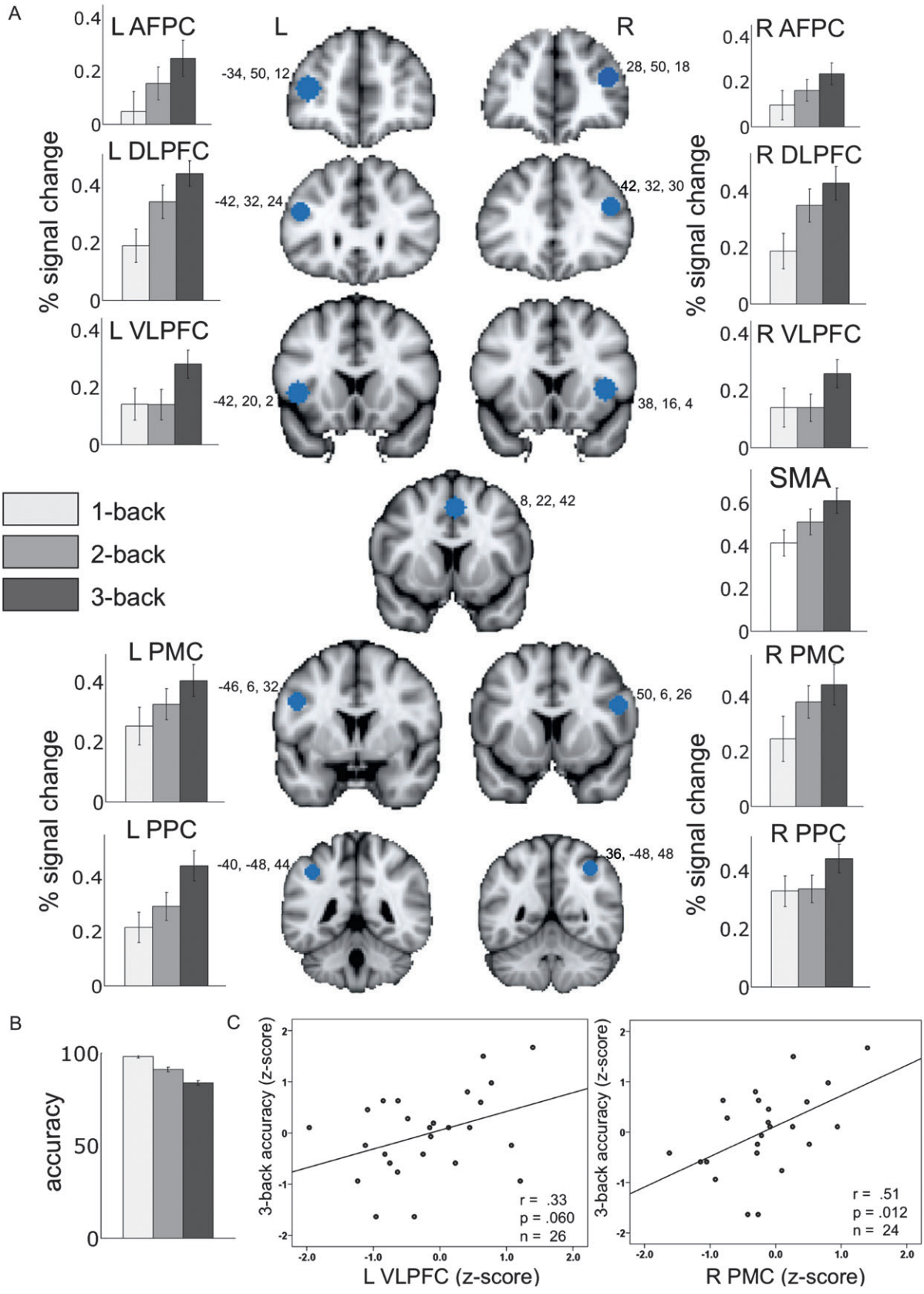

Figure 3. (*A*) BOLD signal change increased across the 3 load levels ($n = 29$). Eight mm spherical ROIs (in blue) are overlaid on a standard anatomical MNI brain. The numbers indicate the MNI coordinates; (*B*) accuracy (% correct) decrease from 1-back to 3-back; error bars: standard error of the mean; (*C*) higher BOLD responsivity (signal change at 3-back minus at 1-back) in R PMC and L VLPFC (*x*-axis) was related to higher 3-back accuracy (*y*-axis).

Table 1
Correlations between SLF FA and BOLD responsivity within cortical regions of the *n*-back functional network

BOLD responsivity	White matter ROI		
	$FA_{L + R SLF}$	$FA_{R SLF}$	$FA_{L SLF}$
L VLPFC	$r = 0.43$, $P = 0.024$, $n = 27$	—	$r = 0.42$, $P = 0.028$, $n = 28$
R VLPFC	$r = 0.40$, $P = 0.041$, $n = 27$	—	$r = 0.39$, $P = 0.038$, $n = 28$
R PMC	$r = 0.53$, $P = 0.006$, $n = 25$	$r = 0.46$, $P = 0.024$, $n = 24$	—
L PMC	—	—	—
L PPC	$r = 0.50$, $P = 0.010$, $n = 26$	$r = 0.47$, $P = 0.016$, $n = 26$	$r = 0.48$, $P = 0.012$, $n = 27$
R PPC	$r = 0.41$, $P = 0.039$, $n = 26$	$r = 0.41$, $P = 0.039$, $n = 26$	—

Note: *r*, Pearson's correlation coefficient; *P*, *P* value; *n*, sample size; —, no significant correlation.

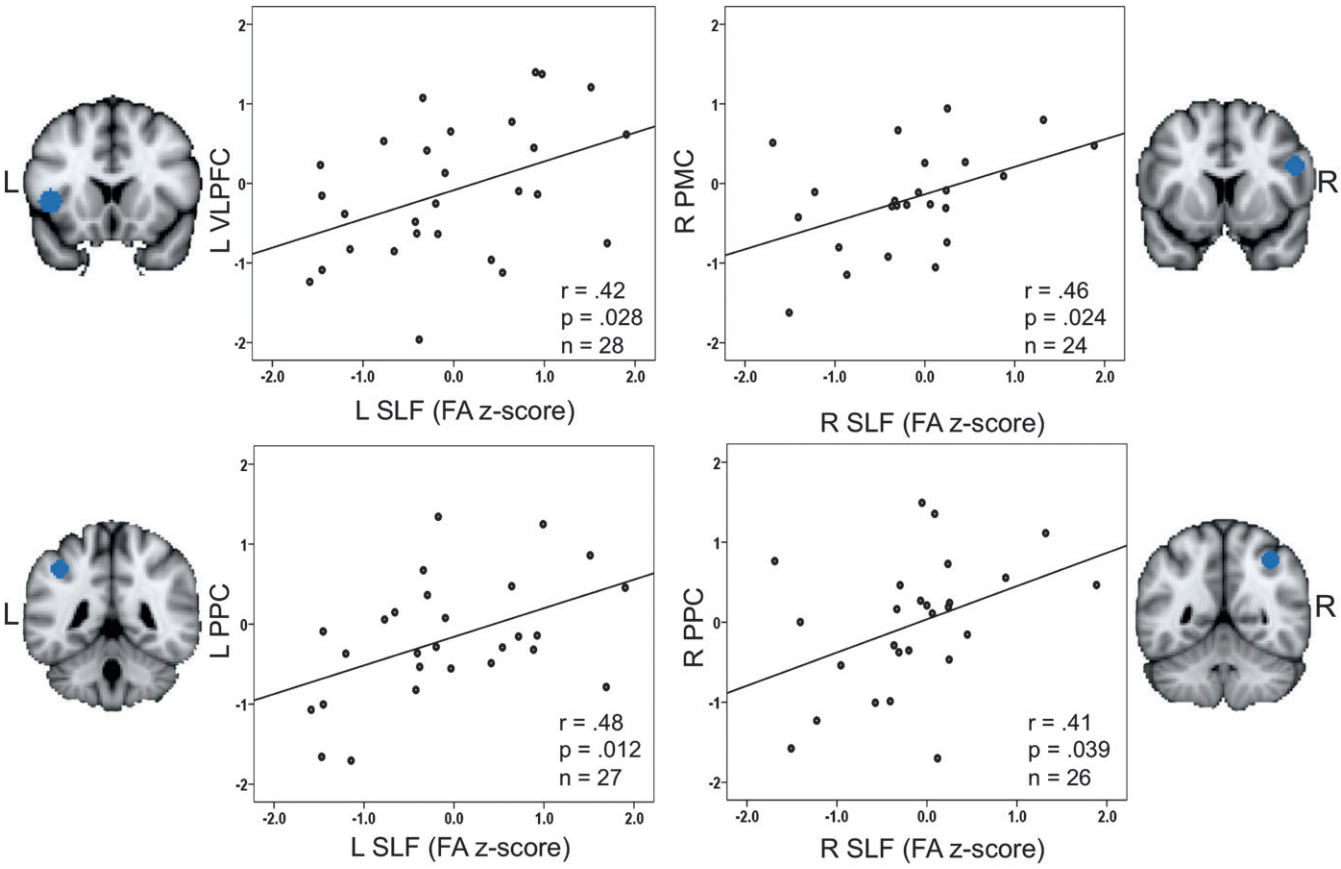

Figure 4. Scatterplots portraying the relations between FA in SLF (*x*-axis) and BOLD responsivity in the L VLPFC, R PMC, as well as L and R PPC (*y*-axis). L: left, R: right.

purpose, we compared 2 multiple regression models; one with FA as the sole predictor and the other with both FA and BOLD responsivity as predictors of WM performance. The hierarchical multiple regression models with FA as the only predictor of 3-back performance yielded: $FA_{L + R SLF}$ $R^2 = 0.188$, $F_{1,22} = 5.09$, $P = 0.034$, and $FA_{R SLF}$ $R^2 = 0.170$, $F_{1,21} = 4.31$, $P = 0.050$. When BOLD responsivity in the R PMC was entered into the model after FA as the second predictor variable, it did not reliably predict additional (i.e., unique) amounts of variance in 3-back performance (model with $FA_{L + R SLF}$: $R^2_{change\ BOLD\ R\ PMC} = 0.098$, $F_{change\ BOLD\ R\ PMC}$ (1/21) = 2.88, $P = 0.105$; model with $FA_{R SLF}$: $R^2_{change\ BOLD\ R\ PMC} = 0.043$, $F_{change\ BOLD\ R\ PMC}$ (1/20) = 1.08, $P = 0.310$).

Discussion

The aim of the present study was to investigate how individual differences in WM microstructure in healthy younger adults are related to BOLD responsivity to increasing WM load within the functional WM network as well as to performance. We tested participants with a verbal *n*-back task with 3 load levels. The key findings were 1) white matter microstructure in frontoparietal connections (SLF) predicted WM performance in young adults; 2) integrity of the SLF was related to greater task-related BOLD responsivity; 3) BOLD responsivity in right PMC satisfied the preconditions to be a mediator of the effect of FA in SLF on WM performance at the highest task demand (i.e., 3-back); and 4) white matter microstructure accounted for the relationship between BOLD responsivity and 3-back performance.

BOLD Responsivity and WM Performance

First, we showed that increasing task demands from 1-back to 3-back resulted in linear reductions in accuracy, confirming that our parametric design successfully manipulated WM demand. Next, we showed that the BOLD signal increased

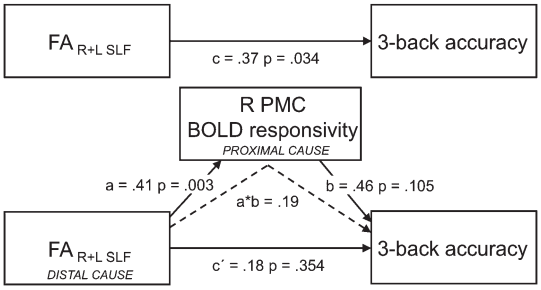

Figure 5. Mediation model: R PMC BOLD responsivity as a mediator of the effect of $FA_{L + R\ SLF}$ on 3-back accuracy. c path: total (direct) effect of $FA_{L + R\ SLF}$ on 3-back accuracy; a path: effect of $FA_{L + R\ SLF}$ on the mediator R PMC BOLD responsivity; b path: effect of the mediator on 3-back accuracy; c′ path: indirect effect of FA on 3-back accuracy through a mediator. a*b: point estimate of the indirect effect of FA on 3-back accuracy mediated by BOLD responsivity (i.e., the multiplication of the paths a and b). The 95% bootstrap confidence intervals of the indirect effect did not contain zero (0.0191, 0.5562), indicating reliable mediation (dashed arrow).

Table 2
Results of the mediation analysis

	Mediation model	
Mediator	R PMC BOLD responsivity	
Independent variable	$FA_{L + R\ SLF}$	$FA_{R\ SLF}$
Sample size	24	23
Coefficients Path a	0 .41, $P = 0.003$	0.35, $P = 0.018$
Path b	0.46, $P = 0.105$	0.29, $P = 0.310$
Path c	0.37, $P = 0.034$	0.37, $P = 0.050$
Path c′	0.18, $P = 0.354$	0.26, $P = 0.207$
Point estimate (bootstrap)	0.187	0.10
95% bootstrap confidence intervals (upper, lower)	0.0191, 0.5662	−0.0213, 0.4545

from 1-back to 3-back in task-relevant regions (bilateral AFPC, DLPFC, VLPFC, SMA, PMC, and PPC), which is in agreement with previous studies (Barch et al. 1997; Braver et al. 1997; Jonides et al. 1997; Klingberg et al. 1997; Manoach et al. 1997; Callicott et al. 1999; Rypma et al. 1999; Nagel et al. 2009, 2010).

In the present sample of healthy young adults, greater increments in the engagement of PMC and, as a trend, left VLPFC with increasing WM load were related to better WM performance at the highest load. Premotor changes in BOLD signal during performing WM are sensitive to task load (Todd and Marois 2005; Leung et al. 2007) and are thought to support information maintenance, manipulation, and attention (Smith and Jonides 1999; Leung et al. 2007). The left VPFC is involved in cognitive control of memory, especially in postretrieval selection during WM (Badre and Wagner 2007). Conceivably, the level of load-dependent BOLD modulation in other regions, such as DLPFC and PPC, was sufficiently high in all participants and, therefore, did not relate to differences in performance.

Individual differences in BOLD responsivity may be due to multiple factors, such as variations in the underlying structural connectivity or in local cortical processing. Specifically, cortical processing is likely to be modulated by variations in neurotransmitter systems, synaptic proteins, and local cortical structure. For instance, Bäckman et al. (2009) showed that age-related changes in dopamine receptor binding account for age-related differences in WM load–induced BOLD responsivity in frontoparietal regions. In a follow-up study, Fischer et al. (2010) simulated cognitive aging by pharmacologically blocking 50% of D1 receptors in young adults, which resulted in both lower WM performance and diminished, old-like BOLD responsivity in young adults. Furthermore, Brassen et al. (2009) showed that the amplitude of the BOLD signal in the PFC is related to local cortical volume among younger adults.

Here, we examined how structural connectivity between functional regions affects BOLD responsivity in these regions and, as a result, WM performance. The present emphasis on white matter microstructure complements previous studies with a focus on gray matter and neurotransmitter systems. Clearly, the interrelations among structural and neurochemical antecedents of neuronal activity and cognitive performance need further study.

SLF Microstructure and WM Performance

We hypothesized that white matter microstructure in the SLF would be related to *n*-back performance as the SLF provides the main route for information transfer between frontal and parietal regions. These regions are robustly activated during *n*-back performance (Jonides et al. 1993, 1997; Miller and Cohen 2001; Owen et al. 2005; D'Esposito 2007; Nagel et al. 2009, 2010).

The SLF FA values reported here were slightly higher than those reported in a recent tractography study (Makris et al. 2005). Our ROI contained only the very core region of the SLF II. Also, TBSS is a more conservative method than the voxelwise analysis used by Makris et al. (2005) because it considers only center-of-tract voxels, which, by definition, have higher FA values. These 2 procedural differences may explain the slight differences in FA values observed in the 2 studies.

As predicted, higher FA in the right and bilateral SLF was related to 3-back accuracy. So far, few studies have demonstrated that interindividual differences in FA relate to behavioral differences in healthy young adults (reaction time (RT) in a visual choice task, Tuch et al. 2005; RT in a bimanual coordination task, Johansen-Berg et al. 2007; RT in a visual target detection task, Madden et al. 2004; proficiency in a mental rotation task, Wolbers et al. 2006; task switching, Gold et al. 2010). In addition, only 3 studies provide evidence for the involvement of frontoparietal white matter connections in WM among healthy adults. First, Karlsgodt et al. (2008) reported that higher FA in the left SLF was related to better verbal auditory WM in 17 young healthy participants. Second, in a sample of older adults (50–90 years) FA in the frontoparietal tracts, composed primarily of the SLF, explained 20.3% of the variance in a composite WM measure (Digit Span Backwards and Letter–Number Sequencing, Wechsler Memory Scale III; Charlton et al. 2008, 2010). Third, 2-month training of WM in young adults resulted in improved performance and increases in FA in the white matter adjacent to the corpus callosum and in parietal regions (Takeuchi et al. 2010).

These findings beg the question how microstructural properties of intact white matter may influence cognitive performance. As a measure of white matter microstructure, FA is a mixture of microscopic (e.g., axon caliber, degree of myelination, and axon density) and macroscopic (alignment of fibers) information within a voxel (Mori 2007). Therefore, higher FA in intact white matter may reflect higher axon volume fraction, higher proportion of large diameter, myelinated, or heavily myelinated axons, smaller axonal spacing, or simply higher coherence of axon alignment within a voxel (Pierpaoli et al. 1996; Beaulieu 2002; Sen and Basser 2005). In our study, we tried to minimize the contribution from the fiber alignment by focusing on the center-of-tract voxels using TBSS. Still, given the limited resolution of our DTI images, it cannot be excluded that

individuals with higher FA had thicker SLF bundles and, therefore, that their center-of-tract voxels were less affected by partial volume with neighboring fibers of different orientation. Taken together, we may assume that higher FA in healthy young individuals reflects mainly differences in microscopic white matter properties. However, given the current level of DTI technology, we are not able to distinguish between differences in myelination, axon caliber, number, or density. All these factors may influence information transfer along a tract: thicker myelin/larger axons facilitate conduction speed and signal synchrony (Fields 2008), and higher axon number allows for parallel information transfer or more fine-tuned signaling. Fast signal transduction may ensure that the information is processed within the temporal retention capacity of the WM network. In other words, if structural connections are less robust, information loss from WM is more likely.

Finally, our finding that the microstructure of the SLF was related to *n*-back performance in younger adults does not exclude the possibility that other white matter pathways may be relevant to WM performance. The white matter–WM associations may depend on the specific WM task or the age composition of the sample (e.g., genu of the corpus callosum and fornix, Zahr et al. 2009; frontotemporal and parietal connections, cingulum, Charlton et al. 2010; anterior corpus callosum, Lövdén et al. 2010).

SLF Microstructure and Cortical Responsivity within the WM Functional Network

FA in the SLF provides a measure for speed or robustness of information transfer between nodes of the WM network, whereas BOLD responsivity reflects the load-related increase in local neural processing. We showed that both white matter microstructure and BOLD responsivity were related to 3-back performance. Finally, the data are consistent with a model according to which greater integrity of white matter tracts interconnecting core WM functional regions are related to greater BOLD responsivity in these regions. The model assumes that structural differences in the ease of communication between cortical regions lead to individual differences in load-dependent responsivity of areas within the WM functional network. This assumption needs further discussion.

At the neuronal level, incoming signals arrive at dendritic spines, and temporal synchronization of these inputs is necessary to reach a critical voltage threshold to trigger an action potential in the recipient neuron. As shown in myelin-deficient rats, myelination was the primary factor in regulation of axon conduction velocity among fibers (Lang and Rosenbluth 2003). Axons differ in their transduction speed to ensure that, regardless of the distance between the neurons, signals arrive at the receiving dendrites within a defined time window (Fields 2008). Speed of signal transduction along the axon is therefore a critical variable in information processing and synaptic function, both within cortical circuits and between distinct regions. For instance, invasive studies on animals demonstrated that conduction times of the input axon are the basis for synchronous complex spike activity in the receiving neurons or neuronal circuits (Sugihara et al. 1993; Baker and Edgley 2006). Therefore, faster signal transduction within the WM network via SLF may be related to more synchronous arrival of multiple synaptic inputs from one cortical region to another, resulting in firing of more action potentials and thus higher BOLD signal and higher cortical responsivity. This potential mechanism is consistent with findings that BOLD mainly reflects synaptic activity and postsynaptic potentials (Logothetis et al. 2001; Goense and Logothetis 2008).

We also found that BOLD responsivity did not account for significant amount of additional variance in WM performance when individual differences in white matter microstructure were taken into account. However, this result must be interpreted with caution. The statistical power to detect unique effects of BOLD responsivity on WM performance was relatively low. It may well be possible that other factors, such as individual differences in vasculature (e.g., D'Esposito et al. 1999) or variations in neurotransmitter systems or molecular synaptic composition (Bäckman et al. 2009; Fischer et al. 2010), contribute to the BOLD signal in more heterogeneous samples, such as older adults. These mechanisms are not mutually exclusive, and all may be shaped by the individual's genetic background and environmental factors (Lindenberger et al. 2008).

It needs to be stressed that the present analyses are correlational in nature. Fitting a mediator model to cross-sectional, nonexperimental data corresponds to a consistency check between theory and data but does not provide a test of the conceptual assumptions that guide the formulation of the statistical model (Lindenberger and Pötter 1998). Thus, the finding that BOLD responsivity mediates the effect of FA on WM performance needs to be corroborated by experimental and longitudinal data. We hope that the present results promote efforts in this direction.

Conclusions

This study demonstrated the importance of a multimodal imaging approach to the study of structure–function–behavior relations. Implementation of this approach was enhanced by parametric variations of task difficulty and the theory-guided selection of white matter tracts. We showed that both interindividual variation in BOLD responsivity and structural connectivity within the frontoparietal network via SLF were related to WM performance in young adults. Moreover, we showed that BOLD responsivity in the R PMC statistically mediated the effect of white matter microstructure on WM performance and that white matter microstructure accounted for the correlational link between BOLD responsivity and WM performance. These results are consistent with the hypothesis that task-related adjustments of local gray matter processing are conditioned by the properties of structural connections between relevant cortical regions. Specifically, we propose that the speed of signal transduction along axons may affect signal summation at neural dendrites, action potential firing, and the resulting BOLD activations. Future studies need to further strengthen the links between structural, neurochemical, and functional properties of the brain, and their interacting and recursive links to behavior (Lindenberger et al. 2006).

Funding

Max Planck Society (the Innovation Fund of the Max Planck Society, M.FE.A.BILD0005); German Federal Ministry for Research to the Berlin NeuroImaging Center (01GO0501);

Deutsche Forschungsgemeinschaft, German Research Council (to H.R.H.), an Alexander von Humboldt Research Award, Swedish Brain Power, and Swedish Research Council (to L.B) and a stipend from the International Max Planck Research School, The Life Course: Evolutionary and Ontogenetic Dynamics (LIFE; to A.Z.B and I.E.N).

Notes

The authors thank the student assistants for their assistance in data collection. Parts of this article were written while U.L. was a fellow at the Center for Advanced Study in the Behavioral Sciences at Stanford University. *Conflict of Interest*: None declared.

References

Achard S, Bullmore E. 2007. Efficiency and cost of economical brain functional networks. PLoS Comput Biol. 3:e17.

Bäckman L, Karlsson S, Fischer H, Karlsson P, Brehmer Y, Rieckmann A, Macdonald SWS, Farde L, Nyberg L. 2009. Dopamine D(1) receptors and age differences in brain activation during working memory. Neurobiol Aging. doi:10.1016/j.neurobiolaging.2009.10.018.

Baddeley A. 2003. Working memory: looking back and looking forward. Nat Rev Neurosci. 4:829–839.

Badre D, Wagner AD. 2007. Left ventrolateral prefrontal cortex and the cognitive control of memory. Neuropsychologia. 45:2883–2901.

Baker MR, Edgley SA. 2006. Non-uniform olivocerebellar conduction time in the vermis of the rat cerebellum. J Physiol. 570:501–506.

Barch DM, Braver TS, Nystrom LE, Forman SD, Noll DC, Cohen JD. 1997. Dissociating working memory from task difficulty in human prefrontal cortex. Neuropsychologia. 35:1373–1380.

Basser PJ. 1995. Inferring microstructural features and the physiological state of tissues from diffusion-weighted images. NMR Biomed. 8:333–344.

Beaulieu C. 2002. The basis of anisotropic water diffusion in the nervous system—a technical review. NMR Biomed. 15:435–455.

Brassen S, Büchel C, Weber-Fahr W, Lehmbeck JT, Sommer T, Braus DF. 2009. Structure-function interactions of correct retrieval in healthy elderly women. Neurobiol Aging. 30:1147–1156.

Braver TS, Cohen JD, Nystrom LE, Jonides J, Smith EE, Noll DC. 1997. A parametric study of prefrontal cortex involvement in human working memory. Neuroimage. 5:49–62.

Callicott JH, Mattay VS, Bertolino A, Finn K, Coppola R, Frank JA, Goldberg TE, Weinberger DR. 1999. Physiological characteristics of capacity constraints in working memory as revealed by functional MRI. Cereb Cortex. 9:20–26.

Charlton RA, Barrick TR, Lawes INC, Markus HS, Morris RG. 2010. White matter pathways associated with working memory in normal aging. Cortex. 46:474–489.

Charlton RA, Landau S, Schiavone F, Barrick TR, Clark CA, Markus HS, Morris RG. 2008. A structural equation modeling investigation of age-related variance in executive function and DTI measured white matter damage. Neurobiol Aging. 29:1547–1555.

D'Esposito M. 2007. From cognitive to neural models of working memory. Philos Trans R Soc Lond B Biol Sci. 362:761–772.

D'Esposito M, Zarahn E, Aguirre GK, Rypma B. 1999. The effect of normal aging on the coupling of neural activity to the bold hemodynamic response. Neuroimage. 10:6–14.

Efron B. 1987. Better bootstrap confidence intervals. J Am Stat Assoc. 82:171–185.

Fields RD. 2008. White matter in learning, cognition and psychiatric disorders. Trends Neurosci. 31:361–370.

Fischer H, Nyberg L, Karlsson S, Karlsson P, Brehmer Y, Rieckmann A, MacDonald SWS, Farde L, Bäckman L. 2010. Simulating neurocognitive aging: effects of a dopaminergic antagonist on brain activity during working memory. Biol Psychiatry. 67:575–580.

Goense JBM, Logothetis NK. 2008. Neurophysiology of the BOLD fMRI signal in awake monkeys. Curr Biol. 18:631–640.

Gold BT, Powell DK, Xuan L, Jicha GA, Smith CD. 2010. Age-related slowing of task switching is associated with decreased integrity of frontoparietal white matter. Neurobiol Aging. 31:512–522.

Hofer S, Frahm J. 2006. Topography of the human corpus callosum revisited–comprehensive fiber tractography using diffusion tensor magnetic resonance imaging. Neuroimage. 32:989–994.

Jenkinson M, Bannister P, Brady M, Smith S. 2002. Improved optimization for the robust and accurate linear registration and motion correction of brain images. Neuroimage. 17:825–841.

Jenkinson M, Smith S. 2001. A global optimisation method for robust affine registration of brain images. Med Image Anal. 5:143–156.

Johansen-Berg H, Della-Maggiore V, Behrens TEJ, Smith SM, Paus T. 2007. Integrity of white matter in the corpus callosum correlates with bimanual co-ordination skills. Neuroimage. 2(36 Suppl):T16–T21.

Jonides J, Schumacher EH, Smith EE, Lauber EJ, Awh E, Minoshima S, Koeppe RA. 1997. Verbal working memory load affects regional brain activation as measured by PET. J Cogn Neurosci. 9:462–475.

Jonides J, Smith EE, Koeppe RA, Awh E, Minoshima S, Mintun MA. 1993. Spatial working memory in humans as revealed by PET. Nature. 363:623–625.

Karlsgodt KH, Erp TGMV, Poldrack RA, Bearden CE, Nuechterlein KH, Cannon TD. 2008. Diffusion tensor imaging of the superior longitudinal fasciculus and working memory in recent-onset schizophrenia. Biol Psychiatry. 63:512–518.

Klingberg T, O'Sullivan BT, Roland PE. 1997. Bilateral activation of fronto-parietal networks by incrementing demand in a working memory task. Cereb Cortex. 7:465–471.

Lang EJ, Rosenbluth J. 2003. Role of myelination in the development of a uniform olivocerebellar conduction time. J Neurophysiol. 89:2259–2270.

Leung H-C, Oh H, Ferri J, Yi Y. 2007. Load response functions in the human spatial working memory circuit during location memory updating. Neuroimage. 35:368–377.

Lindenberger U, Li S-C, Bäckman L. 2006. Delineating brain-behavior mappings across the lifespan: substantive and methodological advances in developmental neuroscience. Neurosci Biobehav Rev. 30:713–717.

Lindenberger U, Nagel IE, Chicherio C, Li S-C, Heekeren HR, Bäckman L. 2008. Age-related decline in brain resources modulates genetic effects on cognitive functioning. Front Neurosci. 2:234–244.

Lindenberger U, Pötter U. 1998. The complex nature of unique and shared effects in hierarchical linear regression: implications for developmental psychology. Psychol Methods. 3:218–230.

Logothetis NK, Pauls J, Augath M, Trinath T, Oeltermann A. 2001. Neurophysiological investigation of the basis of the fMRI signal. Nature. 412:150–157.

Lövdén M, Bodammer NC, Kühn S, Kaufmann J, Schütze H, Tempelmann C, Heinze HJ, Düzel E, Schmiedek F, Lindenberger U. 2010. Experience-dependent plasticity of white-matter microstructure extends into old age. Neuropsychologia 48:3878–3883.

MacKinnon DP. 2000. Contrasts in multiple mediator models. In: Rose JS, Chassin L, Presson CC, Sherman SJ, editors. Multivariate applications in substance use research: New methods for new questions. Mahwah (NJ): Lawrence Erlbaum Associates Publishers. p. 141–160.

MacKinnon DP, Lockwood CM, Williams J. 2004. Confidence limits for the indirect effect: distribution of the product and resampling methods. Multivariate Behav Res. 39:99–128.

Madden DJ, Whiting WL, Provenzale JM, Huettel SA. 2004. Age-related changes in neural activity during visual target detection measured by fMRI. Cereb Cortex. 14:143–155.

Makris N, Kennedy DN, McInerney S, Sorensen AG, Wang R, Caviness VS, Pandya DN. 2005. Segmentation of subcomponents within the superior longitudinal fascicle in humans: a quantitative, in vivo, DT-MRI study. Cereb Cortex. 15:854–869.

Manoach DS, Schlaug G, Siewert B, Darby DG, Bly BM, Benfield A, Edelman RR, Warach S. 1997. Prefrontal cortex fMRI signal changes are correlated with working memory load. Neuroreport. 8:545–549.

Miller EK, Cohen JD. 2001. An integrative theory of prefrontal cortex function. Annu Rev Neurosci. 24:167–202.
Mori S. 2007. Introduction to diffusion tensor imaging. Amsterdam (NL): Elsevier Science.
Mori S, Wakana S, van Zijl PCM, Nagae-Poetscher LM. 2005. MRI atlas of human white matter. Amsterdam (NL): Elsevier Science.
Nagel IE, Preuschhof C, Li S-C, Nyberg L, Bäckman L, Lindenberger U, Heekeren HR. 2009. Performance level modulates adult age differences in brain activation during spatial working memory. Proc Natl Acad Sci U S A. 106:22552–22557.
Nagel IE, Preuschhof C, Li S-C, Nyberg L, Bäckman L, Lindenberger U, Heekeren HR. 2010. Load modulation of BOLD response and connectivity predicts working memory performance in younger and older adults. J Cogn Neurosci. doi:10.1162/jocn.2010.21560.
Nagy Z, Westerberg H, Klingberg T. 2004. Maturation of white matter is associated with the development of cognitive functions during childhood. J Cogn Neurosci. 16:1227–1233.
Nordahl CW, Ranganath C, Yonelinas AP, Decarli C, Fletcher E, Jagust WJ. 2006. White matter changes compromise prefrontal cortex function in healthy elderly individuals. J Cogn Neurosci. 18:418–429.
Olesen PJ, Nagy Z, Westerberg H, Klingberg T. 2003. Combined analysis of DTI and fMRI data reveals a joint maturation of white and grey matter in a fronto-parietal network. Brain Res Cogn Brain Res. 18:48–57.
Owen AM, McMillan KM, Laird AR, Bullmore E. 2005. N-back working memory paradigm: a meta-analysis of normative functional neuroimaging studies. Hum Brain Mapp. 25:46–59.
Petrides M, Pandya DN. 1984. Projections to the frontal cortex from the posterior parietal region in the rhesus monkey. J Comp Neurol. 228:105–116.
Petrides M, Pandya DN. 2002. Comparative cytoarchitectonic analysis of the human and the macaque ventrolateral prefrontal cortex and corticocortical connection patterns in the monkey. Eur J Neurosci. 16:291–310.
Pierpaoli C, Basser PJ. 1996. Toward a quantitative assessment of diffusion anisotropy. Magn Reson Med. 36:893–906.
Pierpaoli C, Jezzard P, Basser PJ, Barnett A, Di Chiro G. 1996. Diffusion tensor MR imaging of the human brain. Radiology. 201:637–648.
Preacher KJ, Hayes AF. 2008a. Asymptotic and resampling strategies for assessing and comparing indirect effects in multiple mediator models. Behav Res Methods. 40:879–891.
Preacher KJ, Hayes AF. 2008b. Contemporary approaches to assessing mediation in communication research. In: Hayes AF, Slater MD, Snyder LB, editors. The Sage sourcebook of advanced data analysis methods for communication research. Thousand Oaks (CA): Sage Publications, Inc. p. 13–54.
Preuss TM, Goldman-Rakic PS. 1989. Connections of the ventral granular frontal cortex of macaques with perisylvian premotor and somatosensory areas: anatomical evidence for somatic representation in primate frontal association cortex. J Comp Neurol. 282:293–316.
Rajah MN, D'Esposito M. 2005. Region-specific changes in prefrontal function with age: a review of PET and fMRI studies on working and episodic memory. Brain. 128:1964–1983.
Reese TG, Heid O, Weisskoff RM, Wedeen VJ. 2003. Reduction of eddy-current-induced distortion in diffusion MRI using a twice-refocused spin echo. Magn Reson Med. 49:177–182.
Rueckert D, Sonoda LI, Hayes C, Hill DL, Leach MO, Hawkes DJ. 1999. Nonrigid registration using free-form deformations: application to breast MR images. IEEE Trans Med Imaging. 18:712–721.
Rypma B, Prabhakaran V, Desmond JE, Glover GH, Gabrieli JDE. 1999. Load-dependent roles of frontal brain regions in the maintenance of working memory. Neuroimage. 9:216–226.
Salmon E, Van Der Linden M, Collette F, Delfiore G, Maquet P, Degueldre C, Luxen A, Franck G. 1996. Regional brain activity during working memory tasks. Brain. 119:1617–1625.
Schlösser RGM, Nenadic I, Wagner G, Güllmar D, von Consbruch K, Köhler S, Schultz CC, Koch K, Fitzek C, Matthews PM, et al. 2007. White matter abnormalities and brain activation in schizophrenia: a combined DTI and fMRI study. Schizophr Res. 89:1–11.
Schmahmann JD, Pandya DN. 2006. Fiber pathways of the brain. New York: Oxford University Press.
Sen PN, Basser PJ. 2005. A model for diffusion in white matter in the brain. Biophys J. 89:2927–2938.
Shing YL, Werkle-Bergner M, Li S-C, Lindenberger U. 2009. Committing memory errors with high confidence: older adults do but children don't. Memory. 17:169–179.
Smith EE, Jonides J. 1999. Storage and executive processes in the frontal lobes. Science. 283:1657–1661.
Smith SM. 2002. Fast robust automated brain extraction. Hum Brain Mapp. 17:143–155.
Smith SM, Jenkinson M, Johansen-Berg H, Rueckert D, Nichols TE, Mackay CE, Watkins KE, Ciccarelli O, Cader MZ, Matthews PM, et al. 2006. Tract-based spatial statistics: voxelwise analysis of multi-subject diffusion data. Neuroimage. 31:1487–1505.
Smith SM, Jenkinson M, Woolrich MW, Beckmann CF, Behrens TEJ, Johansen-Berg H, Bannister PR, Luca MD, Drobnjak I, Flitney DE, et al. 2004. Advances in functional and structural MR image analysis and implementation as FSL. Neuroimage. 1(23 Suppl): S208–S219.
Smith SM, Johansen-Berg H, Jenkinson M, Rueckert D, Nichols TE, Miller KL, Robson MD, Jones DK, Klein JC, Bartsch AJ, et al. 2007. Acquisition and voxelwise analysis of multi-subject diffusion data with tract-based spatial statistics. Nat Protoc. 2:499–503.
Sugihara I, Lang EJ, Llinás R. 1993. Uniform olivocerebellar conduction time underlies Purkinje cell complex spike synchronicity in the rat cerebellum. J Physiol. 470:243–271.
Takeuchi H, Sekiguchi A, Taki Y, Yokoyama S, Yomogida Y, Komuro N, Yamanouchi T, Suzuki S, Kawashima R. 2010. Training of working memory impacts structural connectivity. J Neurosci. 30: 3297–3303.
Todd JJ, Marois R. 2005. Posterior parietal cortex activity predicts individual differences in visual short-term memory capacity. Cogn Affect Behav Neurosci. 5:144–155.
Tuch DS, Salat DH, Wisco JJ, Zaleta AK, Hevelone ND, Rosas HD. 2005. Choice reaction time performance correlates with diffusion anisotropy in white matter pathways supporting visuospatial attention. Proc Natl Acad Sci U S A. 102:12212–12217.
Wolbers T, Schoell ED, Büchel C. 2006. The predictive value of white matter organization in posterior parietal cortex for spatial visualization ability. Neuroimage. 32:1450–1455.
Zahr NM, Rohlfing T, Pfefferbaum A, Sullivan EV. 2009. Problem solving, working memory, and motor correlates of association and commissural fiber bundles in normal aging: a quantitative fiber tracking study. Neuroimage. 44:1050–1062.